

Amino Acid Coated Silver Nanoparticles: A Green Catalyst for Methylene Blue Reduction

Abhishek Chandra, Man Singh

Abstract—Highly stable and homogeneously dispersed amino acid coated silver nanoparticles (ANP) of ≈ 10 nm diameter, ranging from 420 to 430 nm are prepared on AgNO_3 solution addition to gum of *Azadirachta indica* solution at 373.15 K. The amino acids were selected based on their polarity. The synthesized nanoparticles were characterized by UV-Vis, FTIR spectroscopy, HR-TEM, XRD, SEM and $^1\text{H-NMR}$. The coated nanoparticles were used as catalyst for the reduction of methylene blue dye in presence of Sn(II) in aqueous, anionic and cationic micellar media. The rate of reduction of dye was determined by measuring the absorbance at 660 nm, spectrophotometrically and followed the order: $K_{\text{cationic}} > K_{\text{anionic}} > K_{\text{water}}$. After 12 min and in absence of the ANP, only 2%, 3% and 6% of the dye reduction was completed in aqueous, anionic and cationic micellar media respectively while, in presence of ANP coated by polar neutral amino acid with non-polar -R group, the reduction completed to 84%, 95% and 98% respectively. The ANP coated with polar neutral amino acid having non-polar -R group, increased the rate of reduction of the dye by 94, 3205 and 6370 folds in aqueous, anionic and cationic micellar media respectively. Also, the rate of reduction of the dye increased by three folds when the micellar media was changed from anionic to cationic when the ANP is coated by a polar neutral amino acid having a non-polar -R group.

Keywords—Silver nanoparticle, surfactant, methylene blue, amino acid.

I. INTRODUCTION

THE unusual properties of noble metal nanoparticles as compared to their bulk properties has been a field of tremendous interest due to their electronic, optical and antimicrobial properties with applications as catalysts, sensors, bio-probes, drug delivery vehicle and many more [1]-[7]. Among the nanoparticles of noble metals, silver nanoparticles have distinctive optical, electrical, and thermal properties. They are incorporated into products ranging from photovoltaics to biological and chemical sensors. Its high electrical conductivity is utilized for making conductive inks, pastes and fillers while, its novel optical properties is utilized for applications including molecular diagnostics and photonic devices. Its antimicrobial properties are used for antimicrobial coatings in many textiles, wound dressings, and biomedical devices, providing protection against microbes.

The formation, stability, and activity of nanoparticles rely not only on their shape and size controlled distribution, but, also on their synthesis root. Many techniques and methods have been adopted for preparing metallic nanoparticles of

various kind, including polyol processes [8], borohydride reduction [9], solvent extraction–reduction [10], sonochemical methods [11], photolytic reduction [12], radiolytic reduction [13], laser ablation, and microemulsion [14]. However, synthesis of nanoparticles using natural products such as leaf extract, flower extract, seed extract and gum as reducing and capping agents [15]-[20] is one of the most cost effective, environmental friendly and easiest techniques. Nowadays, there is a demand for new synthetic methods, which are environmentally benign, using less harmful chemicals. Thus, we have used neem gum as a reducing, and stabilizing agent for the synthesis of highly stable and small sized silver nanoparticles. We herein report a greener approach for the design and synthesis of water-soluble amino acid coated silver nanoparticles (ANP): AG, AT, AAA and AL with glycine (neutral non-polar), L-tyrosine (neutral polar), L-aspartic acid (acidic polar) and L-lysine (basic polar) respectively. The amino acids were selected based on their polarity, thereby affecting the compactness of the silver nanoparticles internal atomic arrangement. The ANP were used as catalyst for the reduction of cationic dye methylene blue (MB) reduction.

II. MATERIAL AND METHODS

A. Materials

All the chemicals used were of AR grade. The aqueous solution was prepared in double distilled water of $7 \cdot 10^{-7} \text{ S} \cdot \text{cm}^{-1}$ conductivity. Silver nitrate (AgNO_3), methylene blue, glycine, L-tyrosine, L-aspartic acid and L-lysine were purchased from Sigma Aldrich. The neem gum (NG) was collected from neem trees inside the university campus. The crude NG was first dissolved in water and then filtered using Whatmann filter paper. After filtration, the supernatant NG solution was centrifuged at 14000 rpm for 30 min to settle down any big particle. After centrifugation, the NG supernatant was dried at 338.15 K for 48 hrs and the dried product was powdered and used for the reduction of Ag^+ ions into Ag^0 . All chemicals were used as such without any further purification.

B. Synthesis of Silver Nanoparticles Using NG

To a 10 mL 8% (w/v) aq. solution of NG, 10 mL 50 mM aq. solution of AgNO_3 was added drop wise and stirred in dark for 5 min at 1000 rpm. To this, 10 mL 0.1 M aq. amino acid was added drop wise and the solution was further stirred for 5 min at 1000 rpm in dark. The solution was then transferred to a 100 mL RB flask and stirred for 20 min at 500 rpm, maintaining the reaction temperature at 373.15 K. The color of the solution changed from light yellow to dark reddish brown

Abhishek Chandra, Man Singh are with the School of Chemical Sciences, Central University of Gujarat, Sector-30, Gandhinagar-382030, Gujarat, India (phone: +917923260210; fax: +917923260076; e-mail: abhishekchandra.15@gmail.com, mansingh50@hotmail.com).

after 20 min of stirring at 373.15 K indicating the formation of silver nanoparticles. The nanoparticles were extracted from the solution by precipitating with acetone followed by centrifugation at 10,000 rpm for 10 min under cold condition. The precipitates were washed 3-4 times with 50 % aq. acetone and crushed to fine powder after drying at 343.15 K for 24 hrs.

C. Characterization

All spectra were recorded using UV-Vis Spectrophotometer, Spectro 2060 plus, at 298.15 K. The absorbance was measured in 1 cm path length of the quartz crystal cuvette. TEM images were taken with JEOL JEM-2100. A drop of aqueous dispersion of silver nanoparticles was put on the Cu grid and the grid was dried at 338.15 K under vacuum for 1 hr. After complete drying of the grid, TEM image of the nanoparticles was taken. X-ray diffraction was recorded on Bruker, D8 Focus. Lyophilized powder was used to carry out the diffraction experiment. The coating of ANP with amino acids were confirmed from the molecular structure of the NG, amino acids and the synthesized ANP, analyzed by nuclear magnetic resonance spectroscopy (Bruker, 500 MHz NMR) and PerkinElmer Spectrum 65 series FTIR spectrophotometer. The morphological analyses were carried out by using Carl Zeiss Evo-18 SEM.

D. Kinetic Studies for the Reduction of MB Using ANP as Green Catalyst

The reactions were carried out in a 3.5 ml capacity quartz cuvette. 3ml of cationic surfactant DTAB (0.01M) was taken in a quartz cuvette followed by addition of 200 μ L of MB ($5 \cdot 10^{-4}$ M), 100 μ L of SnCl₂ (0.1M) and 50 μ L of 2 % (w/v) of ANP: AG, AT, AAA, AL individually as catalyst. Reaction was carried out at 298.15 K and the color bleaching of the dye

was monitored spectrophotometrically at 660nm for 12 min. For the un-catalyzed reaction, the reactions were carried out in a 3.5 ml capacity quartz cuvette. 3ml of cationic surfactant DTAB (0.01M) was taken in a quartz cuvette followed by addition of 200 μ L MB ($5 \cdot 10^{-4}$ M), 100 μ L SnCl₂ (0.1 M) and 50 μ L water and the color bleaching of the dye was monitored spectrophotometrically at 660nm for 12 min. To study the reduction reaction in water and anionic surfactant SDS, 3 ml of DTAB was replaced with same volume of water and 0.01 M aq. SDS respectively.

III. RESULTS AND DISCUSSION

In our approach of silver nanoparticles synthesis, we have utilized NG as natural green reducing and stabilizing agent, followed by surface coating with amino acids instead of strong reducing agents and chemicals used in traditional methods. The L-arabinose, L-fructose, D-galactose, D-glucuronic acid and traces of D-xylose present in NG not only reduces the silver salt to metallic silver but also acts as a capping agent to avoid the aggregation of silver nanoparticles [21]. The dispersion of the ANP in water was very clear and stable for more than 60 days without settling down, confirming small particle size with no aggregation. The zeta potential of the nanoparticles from DLS analysis (Microtrac Zetatracs, U2771) was found negative with values in the range of -25 mV. To check the stability of the synthesized ANP, their absorbance was monitored for 10 continuous days, which remained constant, thereby confirming no change in size and shape. Fig. 1 illustrates the UV-vis spectra of AT, confirming the amino acid coated surface protect the silver nanoparticles to come close and aggregate, forming bigger size particles.

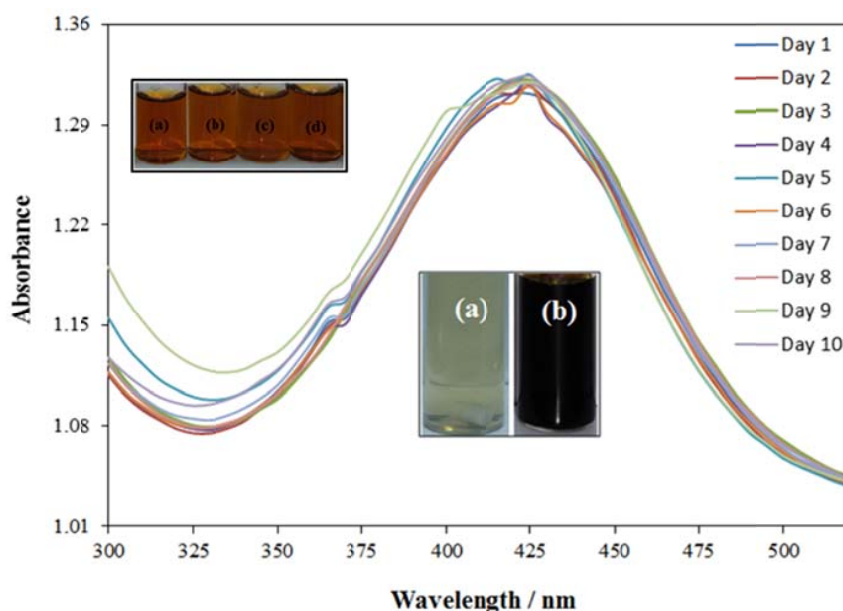


Fig. 1 UV-vis spectra of AT aqueous dispersion from day 1 to 10. Upper inset: digital photograph of ANP: (a) AG, (b) AT (c) AL (d) AAA. Lower inset: (a) NG + AgNO₃ + L-tyrosine aq. mixture at 298.15 K (b) NG + AgNO₃ + L-tyrosine aq. mixture after 20 min stirring at 373.15 K

The TEM images of the ANP are generally spherical in shape with a small fraction of other shapes, with an average size: 4-17 nm. Fig. 2 illustrates the TEM image of AT at 20000X and 800000x magnification, illustrating the

polycrystalline nature of AT from the SAED pattern. The polydispersity index (PDI) of AT, calculated from its TEM image was 0.225 with 8.86 nm average size, having lattice fringe distance of 2.1 Å⁰.

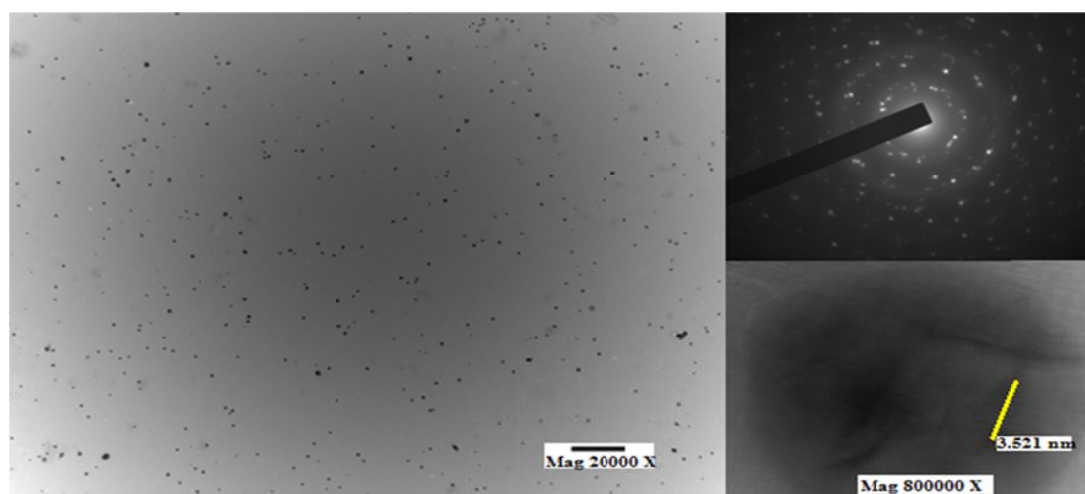


Fig. 2 TEM images of AT. The inset images show polycrystalline nature of AT (SAED pattern), and the lattice fringes

The lattice fringe distance was found to be minimum in case of AT, illustrating that L-tyrosine helped in the formation of a more compact arrangement of silver atoms, thereby increasing the number of Ag⁰ in a fixed area as compared to other amino acid coated surfaces. Fig. 3 shows the SEM image of AT in powdered form. It represents the view of the sample with the magnification of 353 X and solid aggregates could be noticed in range of 500-1000 nm. However, we could not manage to examine the structure of the observed nanoparticles less than this because of difficulties connected with getting higher magnification. These solid aggregates have high homogeneous dispersivity in water confirmed through DLS and TEM images (PDI = 0.225 with 8.86 nm average size).

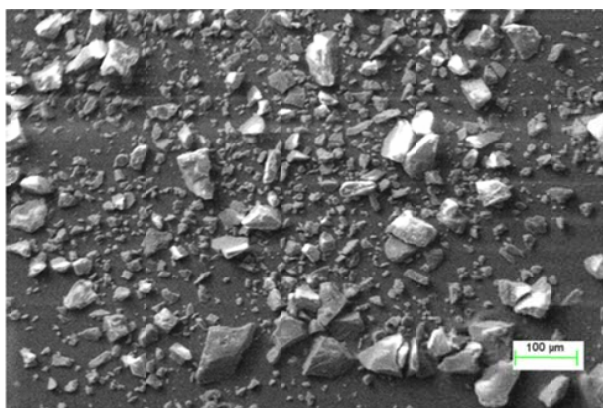


Fig. 3 Scanning electron micrographs of ANP (AT) synthesized with NG and L-Tyrosine

The polycrystalline nature of AT was also confirmed from x-ray diffraction (XRD) analysis. Fig. 4 shows the XRD

pattern of AT with four diffraction peaks at 37.80, 44.20, 64.40 and 77.00 in the 2θ range 20–80° ascribed to the (111), (200), (220) and (311) reflection planes of face-centred cubic (fcc) structure of Ag phases. These diffraction peaks are well consistent with the standard data file JCPDS No 04–0783.

Table I illustrates the rate constants for the reduction of MB in aqueous, anionic and cationic micellar medium using SnCl₂ as reducing agent, and AT having the highest catalytic efficiency. The rate constants followed the order: AT > AL = AAA > AG, AT > AL > AAA > AG and AT > AG > AL > AAA in aq., SDS, and DTAB micellar medium respectively. The rate of MB reduction has been found out to be more in micellar medium than in aqueous medium and follow the trend: K_{DTAB} > K_{SDS} > K_{water}. Figs. 5 and 6 show the catalytic activities of AG, AT, AAA and AL. It was observed that after 3 min and in presence of AT, the reduction completes upto 98, 95 and 60 % in DTAB, SDS and aq. medium respectively. Also, the impact of catalytic efficacy of the nanoparticles can be clearly seen in Figs. 5 and 6, where in absence of the nanoparticles, the reduction of MB in the mediums: aq., SDS and DTAB completes to 0.5, 1 and 1 % in 3 min and 2, 3 and 6 % in 12 min. Thus, SnCl₂, in absence of nanoparticles do not reduces MB remarkably.

The rate constant for the reduction of MB by Sn(II) in presence of only NG and amino acid was also determined. It was found to be of the same order (0.00001 sec⁻¹), as in case of the absence of the ANP (0.00001 - 0.00003 sec⁻¹), which confirmed that AG, AT, AAA and AL were acting as a catalyst and not the L-arabinose, L-fructose, D-galactose, D-glucuronic acid and traces of D-xylose present in NG as well as the amino acids.

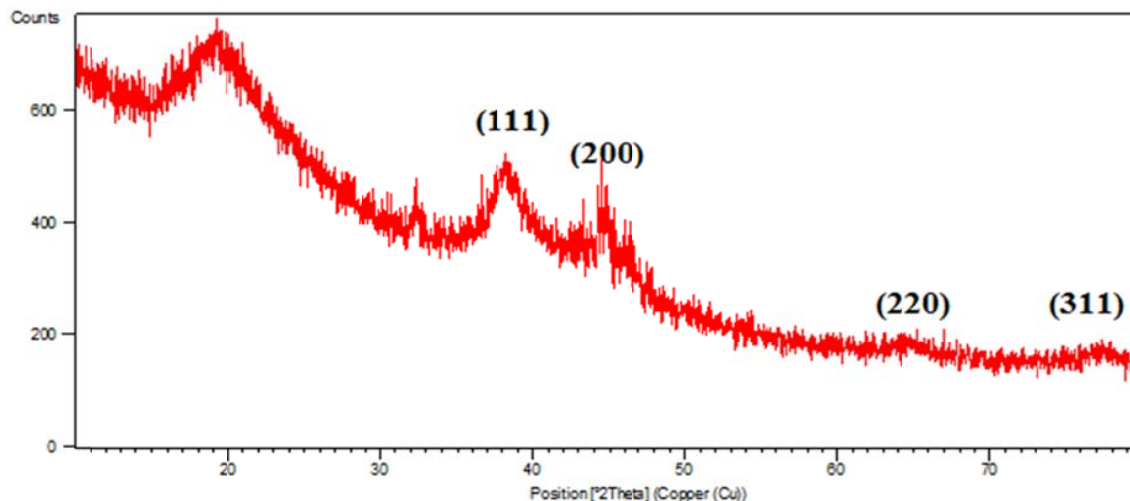


Fig. 4 XRD pattern of silver nanoparticles (AT) synthesized with NG and L-Tyrosine

TABLE I
RATE CONSTANT (K/s^{-1}) OF MB REDUCTION IN PRESENCE OF AG, AT, AL AND AAA NANOPARTICLES AT 298.15 K

Medium	K_{Blank}	K_{AG}	K_{AT}	K_{AL}	K_{AAA}
Aqueous	0.00001	0.00038	0.00094	0.00042	0.00042
0.01 M SDS	0.00002	0.00074	0.06410	0.00158	0.00095
0.01 M DTAB	0.00003	0.00490	0.21020	0.00402	0.00160

The rate of MB color degradation with $SnCl_2$ as a reducing agent was monitored in presence and absence of AT nanoparticles spectrophotometrically at a wavelength of 660 nm in DTAB as a medium, shown in Fig. 7. Fig. 7 (a) shows that the reduction of MB with $SnCl_2$ in absence of AT occurs at an extremely slow rate, indicating that the reaction is very slow under the given time constraint. However, on the addition of AT, Fig. 7 (b), the degradation of MB is greatly enhanced.

In the micellar medium, there is an increase in the frequency of molecular collisions due to the close association of the reactants at the micellar interface [22]. Though $SnCl_2$ is a Lewis base and act as a reducing agent, it cannot reduce MB in the experimental time scale in aqueous and micellar medium. This observation clearly indicates that $SnCl_2$ could not collide effectively with MB molecules under the said experimental condition. However, in a micellar medium, the reduction becomes quantitative because of the increased encounter probability due to the binding of the dye at the micellar surface, resulting in increased molecular collisions with $SnCl_2$. This caused higher rate of MB reduction in micellar medium than in the aqueous. The difference in the rate in cationic and anionic medium is because of the electrostatic interaction between cationic dye (MB) and anionic surfactant (SDS) and because of the electrostatic interaction between the negatively charged ANP surface and the cationic surfactant (DTAB). Table II illustrates the degree of fold increment in rate of MB reduction, in presence of ANP at 298.15 K. The rate is dominated by the highly compact and small sized AT over the other ANP, thereby increasing the rate of MB reduction by more than 3000 and 6000 folds in SDS and DTAB micellar mediums respectively. Thus, along with the nature of the amino acid used for the surface coating, the micellar medium also plays a vital role. When the micellar medium is changed from anionic to cationic, the catalytic activity of AT increased by two folds due to its negative zeta potential and the highly ordered nucleation environment provided by L-tyrosine.

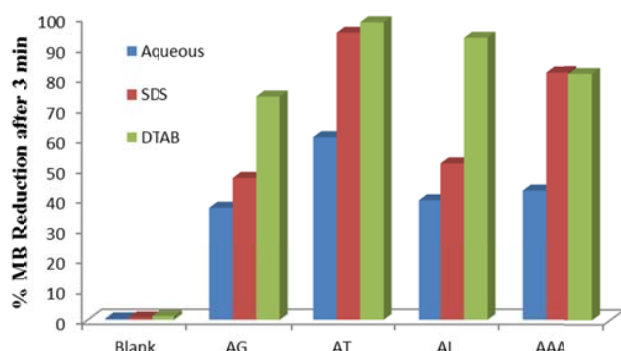


Fig. 5 MB reduction % with ANP as catalyst in aqueous, SDS and DTAB micellar medium at 298.15 K, after 3 min

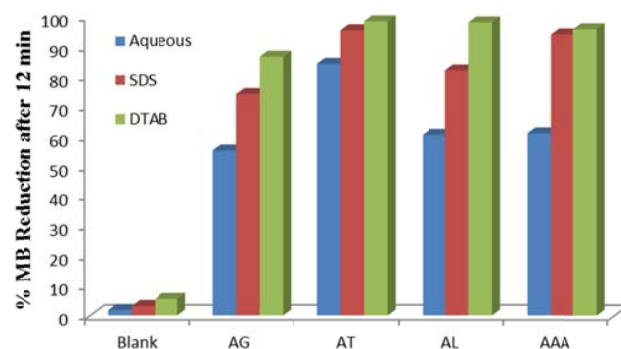


Fig. 6 MB reduction % with ANP as catalyst in aqueous, SDS and DTAB micellar medium at 298.15 K, after 12 min

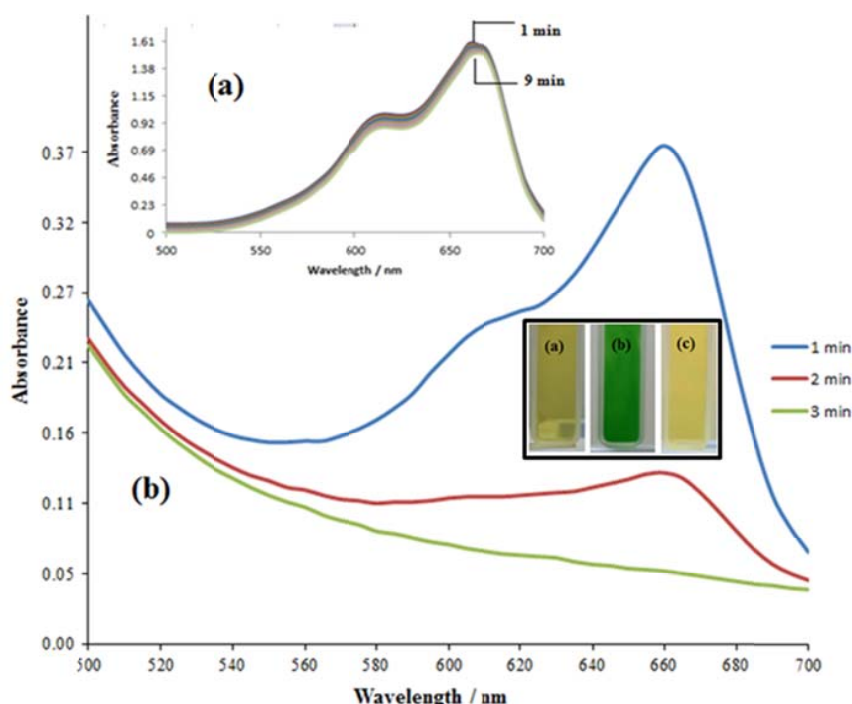


Fig. 7 The decrease in concentration of MB in (a) absence of AT, (b) in presence of AT; inset: (a) AT + SnCl₂ in aq. DTAB, (b) MB + AT + SnCl₂ in aq. DTAB at t = 0 min, (c) MB + AT + SnCl₂ in aq. DTAB at t = 3 min

TABLE II
DEGREE OF FOLD INCREASE IN MB REDUCTION IN AQUEOUS AND MICELLER
MEDIUMS IN PRESENCE OF NANOPARTICLES AT 298.15 K

ANP	Aqueous	0.01 M SDS	0.01 M DTAB
AG	38	37	148
AT	94	3205	6370
AL	42	79	122
AAA	42	47	48

Fig. 8 illustrates the molecular arrangement and possible mechanism of ANP catalytic action in the micellar medium. In case of anionic surfactant SDS, there is an electrostatic interaction between cationic dye (MB) and polar head of anionic surfactant (SDS), while there is electrostatic interaction between cationic head of DTAB and negatively charged ANP surface. Addition of ANP to SDS micellar media result in the adsorption of MB over its surface, which earlier existed as aggregates with less surface area on the micellar surface. This forms a complex micellar surface with increased molecular collisions with SnCl₂. However, in case of cationic surfactant DTAB, the negatively charged ANP surface populates the micellar surface first due to its high surface area by electrostatic interaction with the cationic head of DTAB. The cationic MB then is adsorbed on the surface of ANP by electrostatic interaction. This complex molecular arrangement favors the molecular collisions with SnCl₂, more than with the SDS system leading to highest rate of MB reduction in DTAB medium. The rate of reduction in aq. is extremely slow as compared to SDS and DTAB due to high activation energy and low encounter probability. Due to the

possible mechanism depicted in Fig. 8, the electron transfer takes place easily in DTAB micellar media whereas the interaction prevailing due to the negatively charged ANP surface in SDS micellar media results in the low collision probability. Thus, the rate of MB reduction with faster color bleaching is observed in DTAB as compared to SDS medium.

IV. CONCLUSION

A simple and green method is implemented to prepare amino acid coated silver nanoparticles in a single step using neem gum as reducing and stabilizing agent. The particles are mostly spherical in nature with high monodispersity, having an average size of 10 nm. The nanoparticles were used as catalyst for the reduction of methylene blue in water, cationic and anionic micellar media. The silver nanoparticles coated with L-tyrosine (AT) was found to have the highest catalytic activity over the other nanoparticles on the rate of methylene blue reduction. With all the synthesized silver nanoparticles, the rate of reduction was found to be more in micellar media as compared to aqueous. The rate of MB reduction catalyzed by the ANP was found to be highly influenced by the nature of the micellar medium along with the nature of the amino acid used for surface coating. The encounter probability factors plays the major role in this reduction reaction of MB. The zeta potential of the silver nanoparticles along with the electrostatic forces are the key points for the influence on the encounter probability with Sn (II).

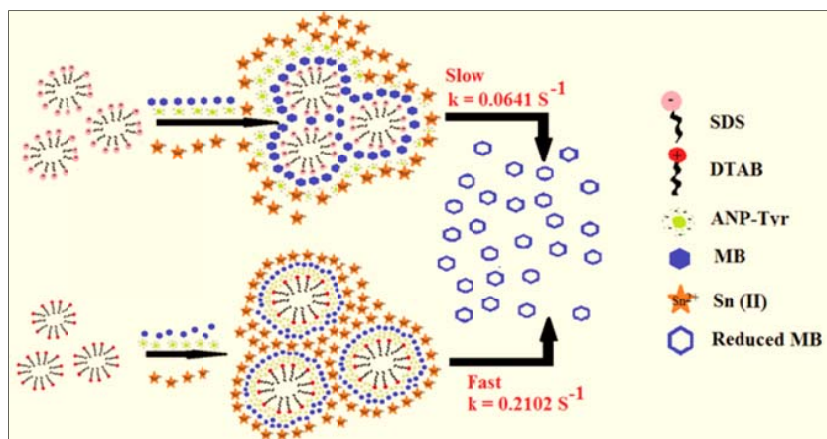


Fig. 8 Molecular arrangement and possible mechanism

ACKNOWLEDGMENT

The Authors are highly thankful to Central University of Gujarat, Gandhinagar, for providing experimental facilities: 500 MHz NMR, HR-TEM, SEM and providing financial support. The authors also like to thank Dr. Dhananjay Mondal and Dr. Smritilekha Bera, School of Chemical Sciences, Central University of Gujarat, for their fruitful suggestions in performing experiments in this study.

REFERENCES

- [1] J.H. He, T. Kunitake, A. Nakao, "Facile in situ synthesis of noble metal nanoparticles in porous cellulose fibers" *Chem. Mater.* vol. 15, pp. 4401-4406, 2003.
- [2] D.D. Evanoff, G. Chumanov, "Synthesis and Optical Properties of Silver Nanoparticles and Arrays" *Chem. Phys. Chem.* vol. 6, pp. 1221-1231, 2005.
- [3] B. Wiley, Y. G. Sun, B. Mayers, Y. N. Xia, "Shape-controlled synthesis of metal nanostructures: The case of silver" *Chem. Eur. J.* vol. 11, pp. 454-463, 2005.
- [4] X. Liu, R. Jin, D. Chen, L. Chen, S. Xing, H. Xing, Y. Xing, Z. Su. "In situ assembly of monodispersed Ag nanoparticles in the channels of ordered mesopolymers as a highly active and reusable hydrogenation catalyst" *J. Mater. Chem. A*, vol. 3, pp. 4307-4313, 2015.
- [5] X. Wang, J. Zhuang, Q. Peng, Y.D. Li "A general strategy for nanocrystal synthesis" *Nature* vol. 437, pp. 121-124, 2005.
- [6] Y. Hamanaka, K. Fukuta, A. Nakamura, L. M. Liz-Marzán, P. Mulvaney, "Enhancement of third-order nonlinear optical susceptibilities in silica-capped Au nanoparticle films with very high concentrations" *Appl. Phys. Lett.* vol. 84, pp. 4938, 2004.
- [7] K.B. Narayanan, N. Sakthivel, "Biological synthesis of metal nanoparticles by microbes" *Adv. Colloid Interface Sci.* vol. 156, pp. 1-13, 2010.
- [8] R. Herpeness, A. Gedanken, "Microwave synthesis of core-shell gold/palladium nanoparticles" *Langmuir* vol. 20, pp. 3431-3434, 2004.
- [9] T. Kim, K. Kobayashi, M. Nagai, "Preparation and characterization of platinum-ruthenium bimetallic nanoparticles using reverse microemulsions for fuel cell catalyst" *J. Oleo Sci.* vol. 56 (10) pp. 553-562, 2007.
- [10] K. Esumi, M. Shiratori, H. Ishizuka, T. Tano, K. Torigoe, K. Meguro, "Preparation of bimetallic palladium-platinum colloids in organic solvent by solvent extraction-reduction" *Langmuir* vol. 7, pp. 457-459, 1991.
- [11] Y. Mizukoshi, K. Okitsu, Y. Maeda, T.A. Yamamoto, R. Oshima, Y. Nagata, "Sonochemical preparation of bimetallic nanoparticles of gold/palladium in aqueous" *J. Phys. Chem. B* vol. 101, pp. 7033-7037, 1997.
- [12] M. Mandal, S. Kundu, S.K. Ghosh, T. Pal, "Micelle mediated UV photoactivation route for the evolution of Pd core-Au shell and Au core-Pd shell bimetallics from photogenerated Pd nanoparticles" *J. Photochem. Photobiol. A: Chem.* vol. 167, pp. 17-22, 2004.
- [13] A. Henglein, "Colloidal palladium nanoparticles: reduction of Pd(II) by H₂; Pd core Au shell Ag shell particles" *J. Phys. Chem.* vol. 104, pp. 6683-6685, 2000.
- [14] M.A. Malik, M.Y. Wani, M.A. Hashim, "Microemulsion method: A novel route to synthesize organic and inorganic nanomaterials" *Arabian J. Chem.* vol. 5, pp. 397-417, 2012.
- [15] D. MubarakAli, N. Thajuddina, K. Jeganathanb, M. Gunasekaran, "Plant extract mediated synthesis of silver and gold nanoparticles and its antibacterial activity against clinically isolated pathogens" *Colloids Surf., B* vol. 85, pp. 360-365, 2011.
- [16] P.S. Ramesh, T. Kokila, D. Geetha, "Plant mediated green synthesis and antibacterial activity of silver nanoparticles using *Emblica officinalis* fruit extract" *Spectrochim. Acta Mol. Biomol. Spectrosc.* vol. 142, pp. 339-343, 2015.
- [17] H.M.M. Ibrahim, "Green synthesis and characterization of silver nanoparticles using banana peel extract and their antimicrobial activity against representative microorganisms" *J. Radiat. Res. Appl. Sci.* vol. 8, pp. 265-275, 2015.
- [18] C.A. Tischer, M. Iacomini, R. Wagner, P.A.J. Gorin, "New structural features of the polysaccharide from gum ghatti (*Anogeissus latifolia*)" *Carbohydr. Res.* vol. 337, pp. 2205-2210, 2002.
- [19] P. Velusamy, J. Das, R. Pachaiappan, B. Vaseeharan, K. Pandian, "Greener approach for synthesis of antibacterial silver nanoparticles using aqueous solution of neem gum (*Azadirachta indica* L.)" *Ind. Crops. Prod.* vol. 66, pp. 103-109, 2015.
- [20] S.S. Shankar, A. Rai, A. Ahmad, M. Sastry, "Rapid synthesis of Au, Ag, and bimetallic Au core-Ag shell nanoparticles using Neem (*Azadirachta indica*) leaf broth" *J. Colloid Interface Sci.* vol. 275, pp. 496-502, 2004.
- [21] S. Mukherjee, H. C. Srivastava, "The Structure of Neem Gum" *J. Am. Chem. Soc.* vol. 77 (2), pp. 422-423, 1955.
- [22] S.K. Ghosh, S. Kundu, M. Mandal, T. Pal, "Silver and Gold Nanocluster Catalyzed Reduction of Methylene Blue by Arsine in a Micellar Medium" *Langmuir*, vol. 18, pp. 8756-8760, 2002.

Abhishek Chandra was born in Patna (Bihar), India on August 15, 1984. He received the B.Sc. degree in Chemistry from Dyal Singh College, University of Delhi, New Delhi, India, in 2006, the M.Sc. degree in Physical Chemistry from Kirori Mal College, University of Delhi, New Delhi, India, in 2009. Presently, he is pursuing his PhD from Central University of Gujarat, Gandhinagar, Gujarat, India, in the group of Prof. Man Singh. His principle research field is focused mainly on the synthesis and application of nanomaterials and the areas involving protein-biochemistry, drug release and delivery, interactions involving biomolecules and surfactants, thermodynamic study on physicochemical properties of solutions, colloid chemistry, protein aggregation, protein-nanoparticle interactions.

Man Singh is a Dean and Professor of the School of Chemical Sciences in the Central University of Gujarat, Gandhinagar, Gujarat, India. Previously, he was a professor of physical chemistry in Deshbandhu College, Delhi University. He completed his Ph.D. in Physical Chemistry in 1987. His research includes the study of molecular engineering, surface chemistry and nanomaterials. He is not only a devoted scientist but also invented several state-of-the-art instruments for measuring physicochemical properties of molecules. Survismeter, Oscosurvismeter, Econoburette and Visionmeter are some of his new inventions, which glorify his dignity as a visionary scientist in the field of world science.